Cauchois–Johansson x-ray spectrograph for 1.5–400 keV energy range

E. O. Baronova[a)] and M. M. Stepanenko
RRC Kurchatov Institute, 123182, Kurchatov Sq. 1, Moscow, Russia

N. R. Pereira
Ecopulse, P.O. Box 528, Springfield, Virginia 22150

(Presented on 22 June 2000)

A Cauchois–Johansson optical scheme is proposed, based on a specially designed cylindrical quartz crystal. The corresponding x-ray spectrograph is manufactured, which provides high spectral resolution in transmission and reflection regimes and covers the wide energy range of 1.5–400 keV. The device is calibrated with an x-ray tube and is suggested to be used in high-temperature plasma diagnostics. © *2001 American Institute of Physics.* [DOI: 10.1063/1.1324754]

I. INTRODUCTION

Focusing x-ray spectrographs of Johann, Johansson, and Cauchois type are successfully used in plasma diagnostics.[1,2] The dispersive elements of these devices are usually quartz, mica, and other crystals, bent cylindrically, spherically, or toroidally. The reflecting crystal planes are parallel to the mechanical crystal surface in Johann geometry, but perpendicular to the surface in Cauchois geometry. Johann and Johansson devices use a reflection geometry appropriate for the softer x rays with photon energy $E<10\,\mathrm{keV}$. These devices need to be in vacuum when $E<5$ keV to prevent the absorption of x rays by air. Cauchois devices use a transmission geometry. They are employed when $E>10\,\mathrm{keV}$ and do not need vacuum. These differing requirements differentiate the design of transmission devices from the ones of reflection type.

This article describes a high-resolution x-ray spectrograph that combines reflection and transmission geometries. The two principal novelties of this device are the Cauchois–Johansson transmission geometry, described later in detail, and the dispersive element. This is a specially designed quartz crystal glued to a cylindrical substrate. The device's vacuum envelope makes the device suitable even for the softest x rays, and allows a wide range of incident angles, 25–75 degrees. Spectra from the x-ray tube are presented, obtained with a single crystal in both the Johansson and the Cauchois–Johansson geometries.

Our Cauchois–Johansson scheme, presented here, to our knowledge, for the first time, provides the important advantages in comparison with the usual Cauchois scheme: the line width does not depend on the size of the x-ray source, and the position of the line does not depend on the position of the source. Therefore the energy and the width of an x-ray line can be determined accurately despite a variation in source size or in its position during the exposure time. This feature is particularly important for x rays from electrical discharges, which are notoriously unstable.

The energy range of our instrument covers the entire range from 1.5 to 400 keV, much wider than for other instruments. The device has high light power and can be effectively used for high-temperature plasma diagnostics.

II. CAUCHOIS–JOHANSSON GEOMETRY AND COMPARISON WITH OTHER TECHNIQUES

We briefly remind the reader here of the traditional Johann, Johansson, and Cauchois optical schemes. Then we describe the Cauchois–Johansson optical scheme, with an emphasis on what is new in comparison with existing instrumentation.

Figure 1(a) shows the optical scheme of the Johann device[3] when measuring the x-ray spectrum emitted by a point source. For simplicity we consider the case of symmetric diffraction from the middle plane of the crystal, and we put the point x-ray source A just on the Rowland circle. X rays are reflected from the crystal K according to Bragg's law $2d\sin\theta = k\lambda$, where $2d$ is twice the interplanar crystal distance, k is the order of reflection, and λ is the wavelength. The spectra are focused on a Rowland circle with radius R.

In the Johann device the radius of the reflecting surfaces of crystal K is equal to $2R$, and the radius of the mechanical crystal surface is $2R$. If the source is just on the Rowland circle, any given wavelength is reflected by all the crystal surfaces. Even if the crystal is perfect and we only consider x rays reflected by the crystal's central planes, the spectral line at the detector position is slightly defocused: B_1 and B_2 do not coincide. This kind of geometrical defocusing is caused by the influence of crystal edges, which lie slightly above the Rowland circle. From the geometry it follows, $\mathrm{arc}\,AB_2 > \mathrm{arc}\,AB_1$, $\mathrm{arc}\,AB_1 = 2R\theta$, $\theta = (\mathrm{arc}\,AB_2 - \mathrm{arc}\,CD)/2R$, and $\mathrm{arc}\,B_1B_2 = \mathrm{arc}\,CD$.

In the Johansson device[4] [see Fig. 1(b)], the radius of the crystal reflecting planes is $2R$, but the radius of the mechanical crystal surface is R. Now the x rays are focused exactly on the detector position: B_1 coincides with B_2 as shown in Fig. 1(b). $\mathrm{Arc}\,AB_1 = \mathrm{arc}\,AB_2 = 2R\theta$ identically, and $\mathrm{arc}\,B_1B_2 = 0$. However, in practice even the best flat crystals are not ideal, and even a single x-ray energy is reflected over a finite angle, the width of the so-called rocking curve. This width is the smallest for a perfect flat crystal. Unfortunately, bending the crystal can double or even quadruple the rocking

[a)]Electronic mail: baranova@nfi.kiae.ru

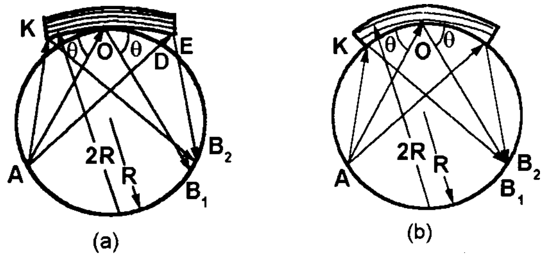

FIG. 1. (a) Johann optical scheme and (b) Johansson optical scheme.

curve's width. Therefore, a spectral line always has a finite width because of this diffraction, and as a result the focusing cannot be perfect: B_1 does not coincide with B_2 in the Johansson device either. Defocusing because of diffraction also happens in Johann devices, but the defocusing from the crystal's curvature and size is always less in the Johansson scheme than in the Johann scheme for identical crystal cuts and whether the crystal is bent cylindrically, spherically, or toroidally.

Figure 2(a) presents the optical scheme of the Cauchois device.[5] Most x rays coming from the extended source A_1A_2 go through the crystal directly, but some are reflected according to Bragg's law. Spectra are focused on the Rowland circle with radius R when the radius of the mechanical crystal surface is equal to $2R$. The crystal reflecting planes are perpendicular to the mechanical crystal surface: the reflecting planes would cross at the same point on the Rowland circle if they were to be extended that far. Focusing of spectral lines in this scheme is not ideal because the crystal edges are not exactly in the right position (geometrical component) and because of diffraction divergence. In this sense the Cauchois optical scheme is similar to the Johann geometry, and we call it here the Cauchois–Johann scheme.

Figure 3(a) illustrates the geometrical defocusing of a spectral line in Cauchois–Johann devices. Point C is the center of the crystal, A is a point on the crystal, and CA is the crystal length reflecting a given wavelength λ at the Bragg angle θ. $D'E'=DE$ is the geometrical defocusing of the line. The angle $\gamma=\mathrm{arc}\,AC/2R$ is a measure of the crystal size, while $\mathrm{arc}\,DE=\alpha R$ measures the line width. From geometrical considerations

$$\alpha=\gamma-\theta+\arcsin\left(\sqrt{5-4\cos\gamma}\,\sin(\theta-\beta)\right),\qquad \sin\beta=\sin\gamma/\sqrt{5-4\cos\gamma} \tag{1}$$

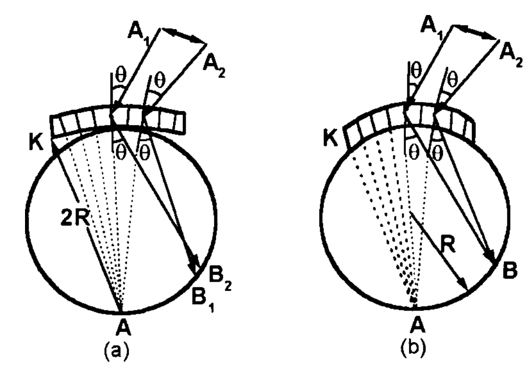

FIG. 2. (a) Cauchois-Johann and (b) Cauchois–Johansson optical schemes.

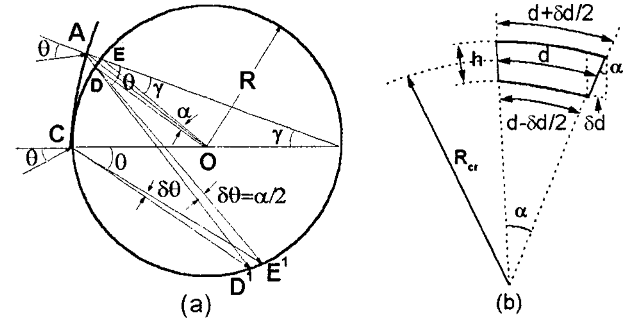

FIG. 3. (a) Geometrical defocusing in Cauchois scheme and (b) influence of δd in Cauchois scheme.

and for small γ we obtain

$$\Delta\theta_{\mathrm{geom}}=(1/2)(\arcsin(5-4\cos\gamma)^{1/2}\sin(\theta-\beta)+\gamma-\theta)$$
$$\cong(\gamma^2/2)(\mathrm{tg}\,(\theta-\gamma)+\gamma)\cong(\gamma^2/2)\,\mathrm{tg}\,\theta\cong(\gamma^2/2)\,\theta, \tag{2}$$

$$(\Delta E/E)_{\mathrm{geom}}=-(\Delta\lambda/\lambda)_{\mathrm{geom}}$$
$$=-(\gamma^2/2)\,\mathrm{ctg}\,\theta(\mathrm{tg}\,(\theta-\gamma)+\gamma)\cong-\gamma^2/2. \tag{3}$$

In analogy with this we estimate the geometrical defocusing for a reflection Johann device:

$$\Delta\theta_{\mathrm{geom}}=(1/2)(\arcsin(5-4\cos\gamma)^{1/2}\cos(\theta-\beta)+\theta-\gamma-\pi/2)$$
$$\cong-(\gamma^2/2)(\mathrm{ctg}\,(\theta-\gamma)-\gamma)\cong-(\gamma^2/2)\,\mathrm{ctg}\,\theta, \tag{4}$$

$$(\Delta E/E)_{\mathrm{geom}}=-(\Delta\lambda/\lambda)_{\mathrm{geom}}$$
$$=-(\gamma^2/2)\,\mathrm{ctg}\,\theta(\mathrm{ctg}\,(\theta-\gamma)-\gamma)$$
$$\cong(\gamma^2/2)\,\mathrm{ctg}^2\,\theta. \tag{5}$$

However, except for geometrical and diffraction defocusing, the device with the bent crystal has the defocusing, caused by change of d after bending. This effect is shown on Fig. 3(b) for a transmission-type crystal. We call h the thickness of the crystal, d, $(d+\Delta d/2)$, and $(d-\Delta d/2)$ the intermediate crystal distance in the middle, outer and inner cross sections respectively, $\Delta d=\alpha h$, and R_{cr} the radius of the crystal. From geometry it follows

$$\Delta d=dh/R_{\mathrm{cr}}. \tag{6}$$

Derivating Bragg equation $2d\sin\theta=\lambda$ under the condition $\delta\lambda=0$ one can obtain

$$\Delta\theta_d=(\Delta d/d)\,\mathrm{tg}\,\theta, \tag{7}$$

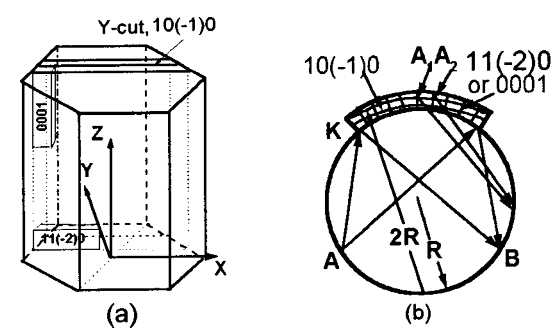

FIG. 4. (a) Quartz crystal and (b) optical scheme with combined crystal.

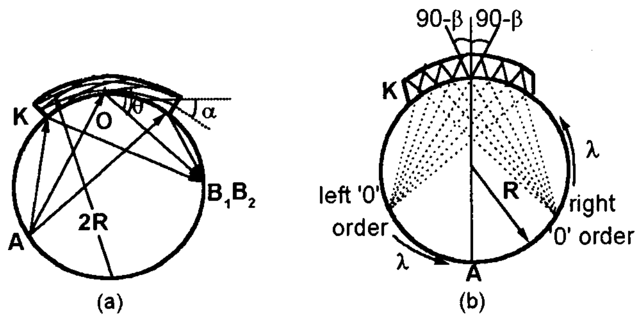

FIG. 5. (a) Asymmetric cuts in reflection scheme and (b) zero orders in transmission scheme with asymmetric cuts.

From (6) and (7) we obtain

$$\Delta \theta_d = (h/R_{\rm cr})\ \mathrm{tg}\ \theta \cong (h/R_{\rm cr})\,\theta. \tag{8}$$

Let us calculate the line width DE for $R=250$ mm and $\theta=30°$ for a Cauchois–Johann device. The typical length of the crystal is 50–70 mm and in the case of extended source the entire crystal surface reflects the line. Therefore the crystals subtends an angle $\gamma=5°$. Using (1) we obtain the geometrical defocusing angle $\alpha=0.004$ rad, so that the line on the detector is $DE=\alpha R \cong 1$ mm wide. This geometrical widening of the line can also reflect an extended source, a broad line, or a point source that moves during exposure. The corresponding geometrical component of resolution $(\Delta\lambda/\lambda)_{\rm geom}=\gamma^2/2\cong 4\times10^{-3}$; it does not depend on θ. The resolution component because of change in d is $(\Delta\lambda/\lambda)_d = \Delta\theta_d\ \mathrm{ctg}\ \theta = h/R_{\rm cr} = 0.7\times10^{-3}$, which also does not depend on θ.

Let us compare the geometrical resolution with an estimated diffraction component. In the best case $\Delta\theta_{\rm diffr} \sim 50$ arcsec for a bent crystal of 250 mm radius.[6] Then $(\Delta\lambda/\lambda)_{\rm diffr} = (\mathrm{ctg}\,\theta)\Delta\theta_{\rm diffr} = 0.4\times10^{-3}$, less than the geometrical component. It is a nontrivial problem to decrease $\Delta\theta_{\rm diffr}$, because this strongly depends on the mechanical distortion of the bent crystal.

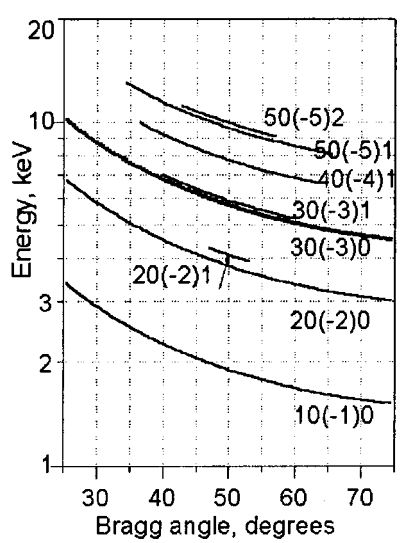

FIG. 6. Energy versus Bragg angle for $10(-1)0$ symmetric cut and very near asymmetric cuts in Johansson geometry. Angle range 25–75 degrees.

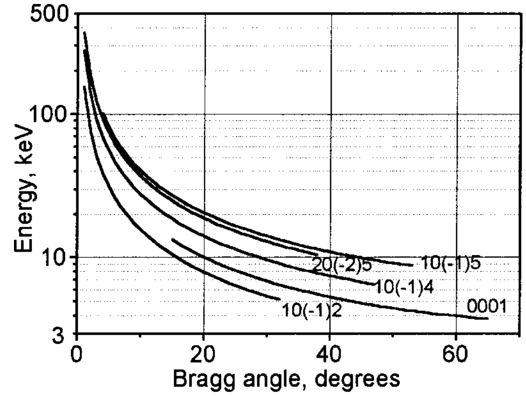

FIG. 7. Energy versus Bragg angle for right orders of 0001 cut and very near asymmetric cuts in transmission geometry. Angle range 25–75 degrees.

We propose the optical scheme in Fig. 2(b) to decrease the geometrical defocusing of lines in transmission geometry. In Fig. 2(b) the mechanical radius of the crystal surface is now equal to R, as in the Johansson scheme. Geometrical continuations of the reflecting planes cross in the same point on the Rowland circle, just as in the Cauchois–Johann scheme. Taking into account these points we call this scheme the Cauchois–Johansson one. In analogy with the Johann and Johansson schemes, the spectral resolution of a Cauchois–Johansson device should be much better than that of a Cauchois–Johann device. It is clearly seen from Fig. 2(b) that $AB=2R\theta$ identically for any arbitrary angle and for all the points along the crystal length. Therefore, the line width does not depend on the source size, and the position of the line does not depend on the position of the source. Geometrical defocusing is zero for the middle plane of the crystal. As always, this statement applies only to an ideal crystal. Resolution depends on the diffraction defocusing of the line and defocusing because of change in d. The art is now to manufacture a crystal that is as close to ideal as humanly possible.

To realize the Cauchois–Johansson scheme we designed and manufactured a quartz crystal 70 mm in length and 10 mm in width, and glued this crystal to a cylindrical substrate with a radius of 250 mm.[7] The crystal can be applied in two ways [see Fig. 4(a)]: with an intermediate distance for symmetric transmission scheme, $d=1.8$ A (0001 cut), and with $d=2.457$ A (11–20 cut). An intermediate distance for a sym-

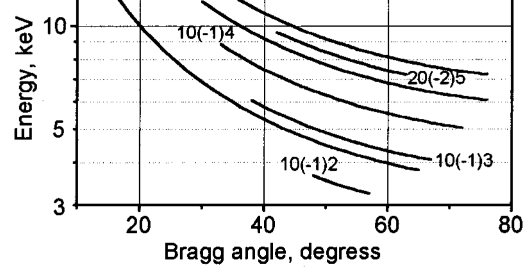

FIG. 8. Energy versus Bragg angle for left orders of 0001 cut and very near asymmetric cuts in transmission geometry. Angle range 25–75 degrees.

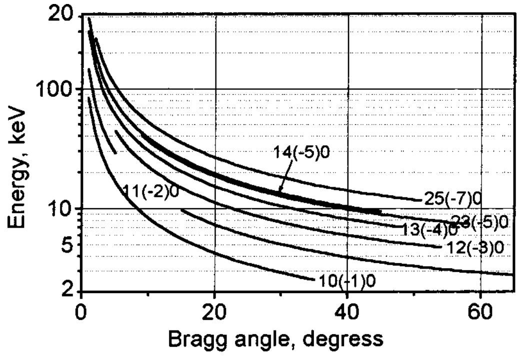

FIG. 9. Energy versus Bragg angle for right orders of $11(-2)0$ cut and very near asymmetric cuts in transmission geometry. Angle range 25–75 degrees.

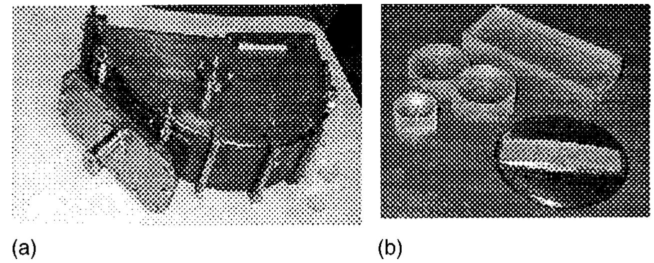

FIG. 11. (a) Photo of device and (b) cylindrical combined crystal and spherical Johansson crystals on optical contact.

metrical reflection scheme is $d = 4.255$ A (10-10 cut) for both cases. This crystal has the following advantages:

(i) It works in transmission Cauchois–Johansson geometry, shown in Fig. 2(b), with the main cut 0001 or $11(-2)0$, and also with a series of asymmetric cuts, given in Figs. 7–10.

(ii) It works in reflection in the Johansson geometry, shown in Fig. 2(b), with the main cut 10-10 and the series of asymmetric cuts given in Fig. 6.

(iii) When the crystal is manufactured with high accuracy, the position of the line does not depend on the position of the source and the width of the line does not depend on the source size for both transmission and reflection schemes.

Figure 4(b) shows the optical scheme with combined crystal. A is an x-ray source, B is the focused line for Johansson geometry, and A_1A_2 is an x-ray source for the Cauchois–Johansson geometry.

Although the manufacturing process of the required crystal is technologically more challenging than that for the simpler Cauchois–Johann crystal, we should mention that similar combined dispersive elements can be done only from quartz, which has high elasticity, mechanical strength, and abundance of cuts with high reflection coefficients.

III. ENERGY RANGE OF THE DEVICE

We analyzed the energy range of the device with the combined Cauchois–Johansson crystal in reflection Johansson scheme, where the symmetric cut of our crystal is $10(-1)0$. Figure 5(a) illustrates the symmetric and asymmetric cuts in the reflection scheme. The angle α is the angle between the given cut and tangent to Rowland circle in point O. For symmetric cuts $\alpha = 0°$. Let us call the angle φ the incident angle with the crystal surface and ϕ the reflected angle with the crystal surface. Than $\varphi = \theta \pm \delta$, $\phi = \theta \mp \alpha$. Figure 6 shows the corresponding plots of energy versus Bragg angle for our crystal, working in Johansson geometry. Energy range of the device in Johansson geometry is 1.5–13.2 keV for angle range 25°–75° and for the series of cuts $10(-1)1$, $20(-2)1$, $30(-3)1$, $40(-4)1$, $50(-5)1$, and $50(-5)2$.

Figure 5(b) shows the zero orders for reflection in the transmission scheme for the Cauchois–Johansson device with a crystal with asymmetric cuts. The zero order is the detector coordinate, corresponding to $\lambda = 0$. We mean that the zero order for the symmetric cut is point A. Each asymmetric cut has its mirror twin due to the inherent symmetry of the quartz crystal. Therefore, left and right zero orders exist for each cut and we show here right and left orders of reflection. The given line can be registered in both orders, if the corresponding incident and reflected angles are accommodated by the device's vacuum envelope and other experimental conditions.

Figures 7 and 8 show the plots of energy versus the Bragg angle for right and left orders for 0001 cut and corresponding asymmetric cuts in transmission geometry. Figures 9 and 10 give the same plots for $11(-2)0$ cut. From those figures the energy range of the device in transmission geometry for 25°–75° angle range is 1.7–400 keV. However, the

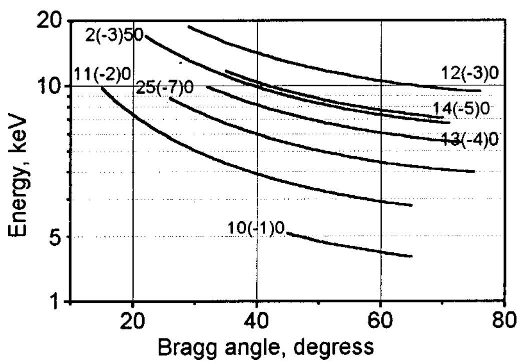

FIG. 10. Energy versus Bragg angle for left orders of $11(-2)0$ cut and very near asymmetric cuts in transmission geometry. Angle range 25–75 degrees.

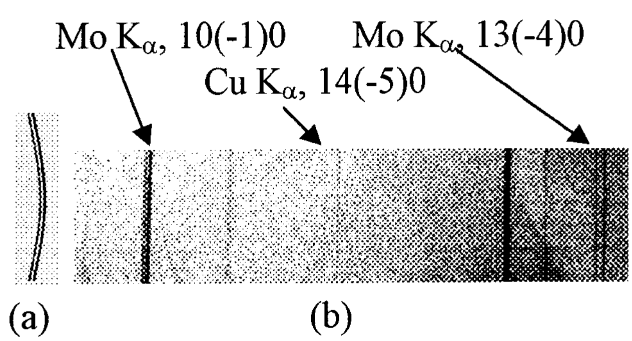

FIG. 12. (a) Cr K_α lines, taken in second order of reflection from $10(-1)0$ cut. (b) Mo K_α lines, taken in the transmission regime in second order of reflection from $10(-1)0$ cut and in first order from $13(-4)0$ cut, Cu K_α lines taken in transmission regime in first order of reflection from $14(-5)0$ cut.

x-ray energy on the low side is limited by absorption inside the crystal. At energies greater than 400 keV spectral resolution is unsatisfied. Therefore, for this device with 0.35 mm thickness crystal, we state a 10–400 keV energy range for the transmission geometry. The total energy range of the device, equipped with our combined crystal, is 1.5–400 keV.

The detailed analysis of the device, given in this section, is important for interpretation of complicated spectra for the choice of the cut with optimal combination of resolution and light power to register lines with the given wavelength and brightness. A similar device is suited for absolutely calibrated measurements of Bremsstrahlung,[8] but in this case it is necessary to use cuts without overlapping of the reflection orders. If the device is calibrated in wavelengths, the heavy ion's velocity can be determined from the Doppler shift.

The device is portable enough [see Fig. 11(a)], and it also accommodates the use of quartz crystals of various cuts, connected to spherical and toroidal substrates by optical contact, shown in Fig. 11(b). This case device provides enough high spatial resolution. Some experimental results on spectral resolution for spherical crystals are given in Ref. 9.

IV. CALIBRATION OF DEVICE

We used a standard x-ray tube with current $I=40\,\mu$A and voltage $U=30\,$kV to verify the operation of the combined Cauchois–Johansson crystal with 11(−2)0, $d=2.457\,$A symmetric transmission cut and 10(−1)0, $d=4.255\,$A symmetric reflection cut. Figure 12(a) shows the Cr K_α spectrum, reflected from the 10(−1)0 cut in the reflection geometry of Fig. 1(b). Lines are visible at 5.4 keV, separated by 0.09 keV, superposed on the bremsstrahlung continuum. Figure 12(b) shows a Mo K_α spectrum at 17.4 keV, separated by 0.105 keV, taken in the transmission geometry of Fig. 2(b). Those spectra are obtained with 13(−4)0 cut and second order of 10(−1)0 cut. This much harder spectrum is also obtained with good precision. The two K-lines are clearly seen at the expected energies of 17.37 and 17.48 keV. We also observed fluorescent Cu K_α lines, 8.047 keV and 8.027 keV, emitted by the border of the x-ray tube and reflected from 14(−5)0 cut. These Cu lines are well resolved, inspite of the fact that the source size is about 7 mm. These experimental results demonstrate that one single crystal can work in transmission and reflection regimes, providing high resolution in both the schemes.

V. CONCLUSIONS

(1) We propose a Cauchois–Johansson optical scheme, which provides higher spectral resolution in the transmission regime than that of the Cauchois-Johann-type scheme.
(2) We have manufactured an x-ray spectrograph with specially designed cylindrical quartz crystal. The crystal works in transmission Cauchois–Johansson geometry with $d=1.8\,$A, cut 0001, or $d=2.457\,$A, cut $11(-2)0$. The same crystal works in reflection Johansson geometry with $d=4.25\,$A, $10(-1)0$.
(3) The energy range of the device was analyzed with accounting of symmetric and asymmetric cuts. The 1.5–400 keV energy range is achieved, which is wider than that of existing prototypes.
(4) Calibration, made with an x-ray tube, showed that one crystal can work in transmission and reflection regimes, providing high spectral resolution in both the schemes. The device is suggested to be used in high-temperature plasma diagnostics.

Presented at the Proceedings of the 13th Topical Conference on High-Temperature Plasma Diagnostics, Tucson, AZ, 18–22 June 2000.

[1] V. A. Boiko, A. V. Vinogradov, S. A. Pikuz, I. U. Skobelev, and A. Y. Faenov, Itogi nauki i techniki **27**, (1980).
[2] B. S. Fraenkel and M. Bitter, Rev. Sci. Instrum. **70**, 296 (1999).
[3] H. H. Johann, Z. Phys. **69**, 185 (1931).
[4] T. Johansson, Naturwissenschaften **3**, 320 (1932).
[5] Y. Cauchois, J. Phys. **3**, 320 (1932).
[6] V. V. Lider, E. O. Baronova, and M. M. Stepanenko, Crystallography (to be published).
[7] E. O. Baronova, M. M. Stepanenko, V. V. Lider, and N. R. Pereira, Proc. of Second Workshop Conf. on Curved Crystal X-ray Optics, Weimar (1999).
[8] E. O. Baronova, V. A. Rantsev-Kartinov, and M. M. Stepanenko, in Proceedings Beams 98 Conference, edited by M. Marcovits and J. Shiloh, 1998, Vol. 2, p. 572.
[9] M. M. Stepanenko and E. O. Baronova, Instrum. Exp. Tech. **42**(5), 1 (1999).